

Interestingly, as with mice lacking Dok-7, Lrp4-deficient mice do not show MuSK-dependent muscle pre patterning or NMJ formation (20), suggesting that both Dok-7 and Lrp4 are required for MuSK activation under physiological conditions, in contrast to our observation that Dok-7 can activate MuSK in the absence of Lrp4 or its ligand agrin, at least in vitro (19). Thus, we examined if Dok-7 can activate MuSK in the absence of Lrp4 or agrin in vivo and compensate for their deficiency in the formation and/or maintenance of NMJs.

Results

Forced Expression of Dok-7 Activates MuSK in Agrin-Deficient Mice.

Although agrin is expressed in both motor neurons and myotubes, only the nerves produce an alternatively spliced isoform called “z-agrin,” which is solely responsible for agrin-mediated activation of MuSK (9, 21, 22). MuSK activity has been widely monitored both in vivo and in vitro through tyrosine phosphorylation of MuSK itself or “autophosphorylation,” including studies on z-agrin- and Dok-7-mediated activation of MuSK. Although not all phosphorylation sites necessarily correlate with kinase activity, this potentially imperfect surrogate provides a high degree of sensitivity. To address whether Dok-7 can activate MuSK in the absence of z-agrin (hereafter “agrin”) in vivo, we crossed agrin-deficient mice with Dok-7 transgenic (Tg) mice, in which MuSK is strongly activated due to forced skeletal muscle-specific expression of Dok-7 tagged with enhanced green fluorescent protein (EGFP) (9, 19). We previously demonstrated that Dok-7 activates MuSK in cultured myotubes in the absence of agrin (17, 18) and thus anticipated similar strong activation of MuSK in Dok-7 Tg mice that lack agrin. Indeed, the level of MuSK phosphorylation was comparable in the skeletal muscle of Dok-7 Tg embryos with or without agrin at embryonic day 18.5 (E18.5) (Fig. 1 *A* and *B*), when agrin is indispensable for NMJ formation in wild-type (WT) embryos (9). By contrast, MuSK phosphorylation was undetectable in WT or agrin-deficient embryos, as also reported by others (25), suggesting that the endogenous, physiological level of MuSK phosphorylation is not

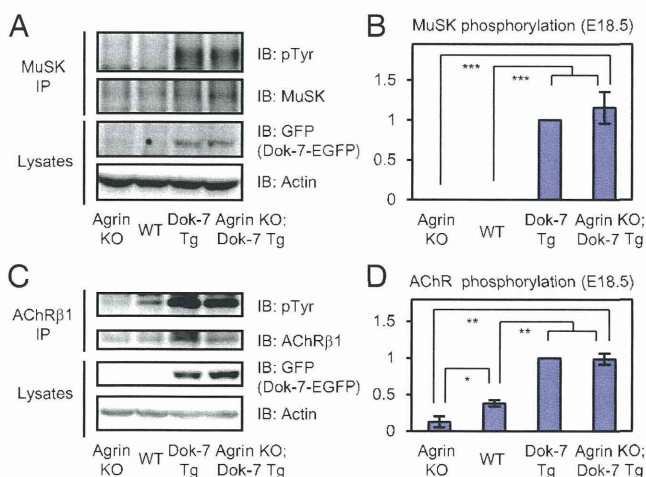


Fig. 1. Forced expression of Dok-7 activates MuSK in agrin-deficient mice. (*A* and *C*) The limb-muscle lysates and anti-MuSK or anti-AChR β 1-subunit (AChR β 1) immunoprecipitates (IPs) from the lysates of wild-type (WT), Agrin KO, Dok-7 Tg, or Agrin KO; Dok-7 Tg embryos at E18.5 were subjected to immunoblotting (IB) with the indicated antibodies. pTyr, phosphotyrosine. (*B* and *D*) Ratio of tyrosine phosphorylation of MuSK or AChR to total amount of each protein was quantified. The relative intensity of MuSK or AChR phosphorylation in Dok-7 Tg was arbitrarily defined as 1. Error bars indicate mean \pm SD ($n = 3$). Asterisks denote significant statistical difference: * $P < 0.05$, ** $P < 0.01$, *** $P < 0.001$.

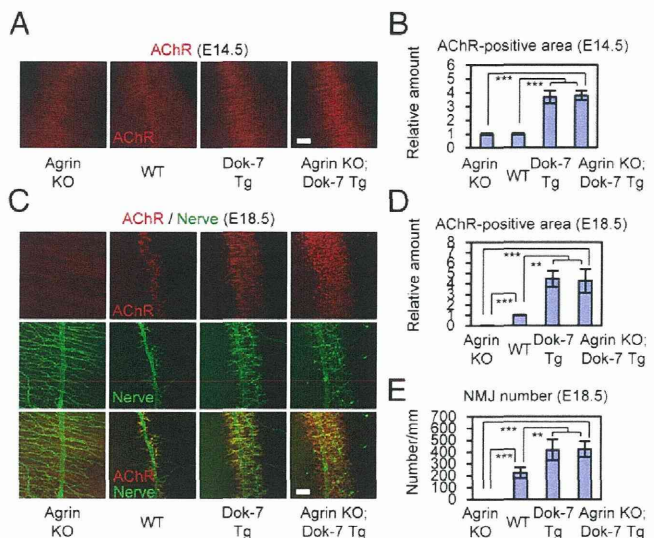


Fig. 2. Forced expression of Dok-7 restores NMJ formation in agrin-deficient mice. (*A* and *C*) Diaphragm muscles of WT, Agrin KO, Dok-7 Tg, or Agrin KO; Dok-7 Tg embryos at E14.5 (*A*) or E18.5 (*C*) were stained with Btx (AChR) and/or antibodies to neurofilament and synaptophysin (“Nerve”). (*B*, *D*, and *E*) The AChR-positive area at E14.5 (*B*) or E18.5 (*D*) and the number of NMJs at E18.5 (*E*) were quantified. The mean value of the AChR-positive area in WT was arbitrarily defined as 1. Error bars indicate mean \pm SD. Data were collected from three or more diaphragm muscles for each genotype. Asterisks denote significant statistical difference: ** $P < 0.01$ and *** $P < 0.001$. (Scale bars, 100 μ m.)

detectable with the methods used in these studies. However, phosphorylation of AChR, which is triggered on activation of MuSK (26), was decreased compared with WT, but nevertheless detectable in agrin-deficient embryos, reflecting Dok-7-mediated activation of MuSK (19) (Fig. 1 *C* and *D*). In addition, this phosphorylation was greatly elevated in Dok-7 Tg embryos irrespective of agrin. These results indicate that forced expression of Dok-7 in vivo induces robust activation of MuSK in the absence of agrin.

Forced Expression of Dok-7 Restores NMJ Formation in Agrin-Deficient Mice.

As mentioned earlier, agrin is required for NMJ formation, but not for muscle pre patterning of postsynaptic specializations. Consistent with this, the lack of agrin did not affect prominent AChR clustering in the correct central region of myotubes at E14.5 before neuromuscular synaptogenesis, and forced expression of Dok-7 enhanced the pre patterning as we previously demonstrated (19) (Fig. 2 *A* and *B*). In accordance with an essential role for agrin in the preservation of postsynaptic specialization upon motor innervation at E18.5 when NMJs are normally formed in the central region of myotubes in WT embryos, only a few small AChR clusters were present and distributed throughout myotubes in agrin-deficient embryos as previously reported (8, 9) (Fig. 2 *C* and *D*). However, forced expression of Dok-7 in agrin-deficient embryos facilitated AChR clustering in the central region of muscle. Furthermore, visualization of motor axons and presynaptic nerve terminals revealed that Dok-7 Tg mice developed a significantly greater number of NMJs than the WT controls not only in the presence of agrin, as previously described (19), but also in the absence of it (Fig. 2 *C* and *E* and Fig. S1). Consistent with this, forced expression of Dok-7 in the skeletal muscle rescued all agrin-deficient mice from neonatal lethality. Together, these findings indicate that the exogenous Dok-7-mediated activation of MuSK compensates for agrin deficiency in prenatal NMJ formation.

Lrp4 Is Required for Efficient Activation of MuSK by Dok-7 in Vivo. We previously purified bacterially expressed Dok-7 and the cytoplasmic region of MuSK (MuSK-cyt) including the kinase domain and showed that Dok-7 can directly activate the kinase in vitro (19). We also demonstrated that forced expression of either MuSK or MuSK-cyt alone did not result in activation of the expressed kinase, but did with forced and simultaneous expression of Dok-7 in HEK293T cells (17–19). However, muscle pre patterning is dependent not only on Dok-7 and MuSK, but also on Lrp4 (20), raising the possibility that in skeletal muscle Dok-7 might not be able to activate MuSK without Lrp4 also present. Thus, we crossed Dok-7 Tg mice with Lrp4-deficient mice (20) and found that forced expression of Dok-7 in the muscle induces MuSK activation in mice lacking Lrp4 as judged by MuSK and AChR phosphorylation (Fig. 3 and Fig. S2). However, the phosphorylation level of MuSK in Dok-7 Tg embryos lacking Lrp4 was significantly lower than that in Dok-7 Tg embryos with intact Lrp4 at both E14.5 and E18.5 (Fig. 3 *A* and *B* and Fig. S2 *A* and *B*). Together, these data indicate that Lrp4 is required for efficient activation of MuSK by Dok-7 in the muscle. Although AChR phosphorylation was detectable at E14.5 only in Dok-7 Tg embryos with intact Lrp4 (Fig. S2 *C* and *D*), its phosphorylation in Lrp4-deficient Dok-7 Tg embryos at E18.5 was detectable and comparable to that in WT embryos (Fig. 3 *C* and *D*), in which MuSK phosphorylation was undetectable and thus weaker than that in Lrp4-deficient Dok-7 Tg embryos (Fig. 3 *A* and *B*). This implies that Lrp4 may also play an important role in MuSK-dependent phosphorylation of AChR.

Forced Expression of Dok-7 Restores Muscle Pre patterning but Not NMJ Formation in Lrp4-Deficient Mice. Because forced expression of Dok-7 activates MuSK in the absence of Lrp4, we examined if it restores muscle pre patterning in Lrp4-deficient embryos. Indeed, forced expression of Dok-7 in Lrp4-deficient embryos promoted substantial AChR clustering in the central region of the muscle at E14.5 (Fig. 4 *A* and *B*). However, probably due to the decreased level of MuSK activation mentioned above, AChR clustering was less pronounced in Dok-7 Tg mice lacking Lrp4 than in those with intact Lrp4. Furthermore, these AChR clusters were not maintained, and NMJ formation occurred, but was

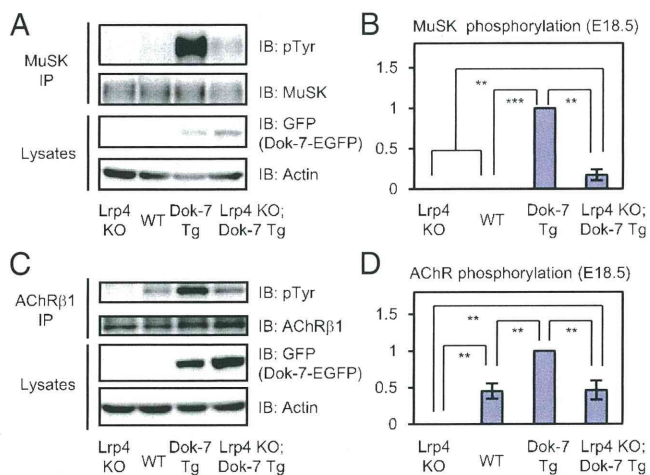


Fig. 3. Lrp4 is required for efficient activation of MuSK by Dok-7 in vivo. (A and C) The limb-muscle lysates and anti-MuSK or anti-AChR β 1 IP from the lysates of WT, Lrp4 KO, Dok-7 Tg, or Lrp4 KO;Dok-7 Tg embryos at E18.5 were subjected to IB with the indicated antibodies. (B and D) Ratio of tyrosine phosphorylation of MuSK or AChR to total amount of each protein was quantified. The relative intensity of MuSK or AChR phosphorylation in Dok-7 Tg was arbitrarily defined as 1. Error bars indicate mean \pm SD ($n = 3$). Asterisks denote significant statistical difference: ** $P < 0.01$ and *** $P < 0.001$.

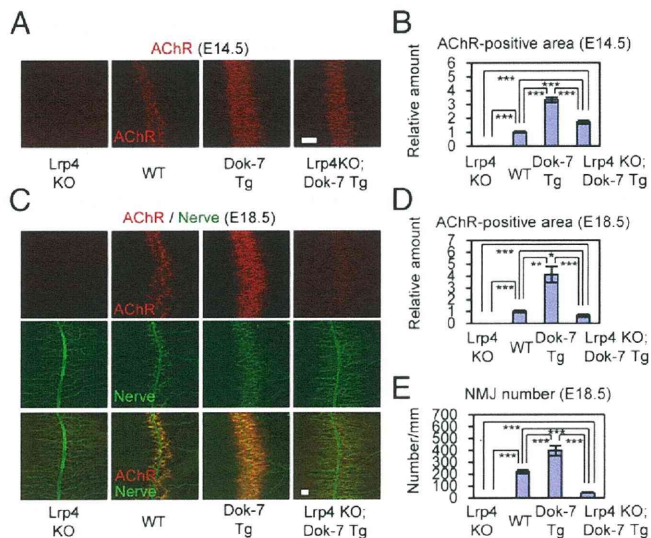


Fig. 4. Forced expression of Dok-7 restores muscle pre patterning but not NMJ formation in Lrp4-deficient embryos. (A and C) Diaphragm muscles of WT, Lrp4 KO, Dok-7 Tg, or Lrp4 KO;Dok-7 Tg embryos at E14.5 (A) or E18.5 (C) were stained with Btx (AChR) and/or antibodies to neurofilament and synaptophysin (“Nerve”). (B, D, and E) The AChR-positive area at E14.5 (B) or E18.5 (D) and the number of NMJs at E18.5 (E) were quantified. The mean value of the AChR-positive area in WT was arbitrarily defined as 1. Error bars indicate mean \pm SD. Data were collected from three or more diaphragm muscles for each genotype. Asterisks denote significant statistical difference: * $P < 0.05$, ** $P < 0.01$, *** $P < 0.001$. (Scale bars, 100 μ m.)

severely impaired at E18.5 in Lrp4-deficient embryos despite the presence of the Dok-7 transgene (Fig. 4 *C–E* and Fig. S3). Unlike Lrp4-deficient mice, which cannot move due to the lack of NMJs, those with the Dok-7 transgene were able to move for at least 10 min after birth, but died within 1 h, indicating the presence of severely impaired, but marginally functional NMJs at birth. Given that MuSK phosphorylation in Lrp4-deficient Dok-7 Tg embryos was greater than that in the WT controls at E18.5 (Fig. 3 *A* and *B*), these data suggest that Lrp4 plays a role distinct from MuSK activation in the maintenance of postsynaptic specialization in embryonic skeletal muscle. Consistent with this idea, it was recently demonstrated that Lrp4 plays an essential role as a retrograde signal in presynaptic differentiation of motor neurons (27, 28), raising the possibility that as-yet-undefined signaling from presynaptic nerve terminals, which are lost in Lrp4-deficient embryos, is required for the maintenance of AChR clusters after motor innervation during normal development.

Agrin Is Required for the Postnatal Maintenance of NMJs Irrespective of MuSK Activation. Although forced expression of Dok-7 via a transgene restored embryonic NMJ formation and neonatal survival in all agrin-deficient mice, we found that these mice survived no longer than 8 wk after birth (Fig. S4A). However, Dok-7 Tg mice with intact agrin survived more than 1 y after birth (Fig. S4B), indicating forced expression of Dok-7 has no lethal pathogenic effects. By 5 wk of age, Dok-7 Tg mice lacking agrin, but not those with intact agrin, exhibited severe motor defects; they were required at least 30 s to right themselves after being placed on their side and showed greatly reduced motor performance in rotarod tests (Fig. S5). They also showed abnormal curvature of the spine between the thoracic and lumbar vertebrae (thoracolumbar kyphosis), indicating a myasthenic phenotype (Fig. S6). Indeed, histological examination of the diaphragm muscle revealed that NMJs in Dok-7 Tg mice were much less numerous in the absence than in the presence of agrin at 5 wk of

age, whereas the number of NMJs was comparable in Dok-7 Tg mice at birth [postnatal day 0 (P0)] and 1 wk of age irrespective of agrin (Fig. 5 A–D). These results raise the possibility that MuSK activation might be impaired due to the lack of agrin in the mutant mice. However, even at 5 wk of age, the phosphorylation levels of MuSK and AChR were each comparable in Dok-7 Tg mice irrespective of the presence or absence of agrin and was significantly higher than that in WT mice, confirming that the exogenous Dok-7-mediated activation of MuSK was maintained until at least 5 wk of age (Fig. 5 E and F and Fig. S7). Thus, we further investigate the size of AChR clusters together with the cover ratio of presynaptic nerve terminals at NMJs to delineate defects in agrin-deficient Dok-7 Tg mice compared with NMJs in Dok-7

Tg mice with intact agrin. We found that both parameters were comparable irrespective of agrin at P0, but were lower in the absence than in the presence of agrin at 1 wk of age (Fig. S8). Interestingly, the coverage of presynaptic nerve terminals over AChR clusters, but not the size of the clusters, further decreased at 5 wk of age only in the absence of agrin, indicating an apparent defect in motor innervation (Fig. 5G and Fig. S8). Also, we found that the cover ratio at NMJs was lower in Dok-7 Tg mice than in WT mice even at P0 (Fig. S8B). Because the size of postsynaptic AChR clusters had already begun to enlarge at P0 in Dok-7 Tg mice compared with WT mice (Fig. S8A), this is probably due to lagging enlargement of presynaptic nerve terminals in response to the enlarged AChR clusters in the muscle.

In addition to the NMJ defects, we also found that small AChR clusters formed uniformly throughout myotubes in agrin-deficient Dok-7 Tg mice (Fig. S9), suggesting noncentral, ectopic expression of MuSK because AChRs cluster where MuSK is expressed in the muscle (29). Indeed, the midmuscle-restricted expression of *MuSK* transcripts was lost, and instead their uniform expression was observed in Dok-7 Tg mice in the absence but not in the presence of agrin (Fig. 5H). Also, the loss of midmuscle-restricted expression of *AChR α* transcripts, which is known to be dependent on MuSK (5), was confirmed in agrin-deficient Dok-7 Tg mice (Fig. S10A). By contrast, these transcripts were correctly restricted to the central region of muscle at E18.5 in agrin-deficient Dok-7 Tg embryos (Fig. S10B). Furthermore, because (i) Dok-7 Tg mice showed enhanced NMJ formation, compared with WT mice, in the correct central region of myotubes before and after birth and (ii) agrin-deficient Dok-7 Tg embryos also showed enhanced midmuscle NMJ formation (Figs. 2, 4, and 5 and Figs. S1, S3, S9, and S10), it is unlikely that forced expression of Dok-7 per se causes disassembly of NMJs and formation of small AChR clusters universally throughout myotubes in agrin-deficient Dok-7 Tg mice after birth, although nonphysiological effects of the transgene are not completely excluded. Together, these findings demonstrate that agrin plays an essential role distinct from MuSK activation in the postnatal maintenance of NMJs as well as in the postnatal, but not prenatal, midmuscle expression of MuSK.

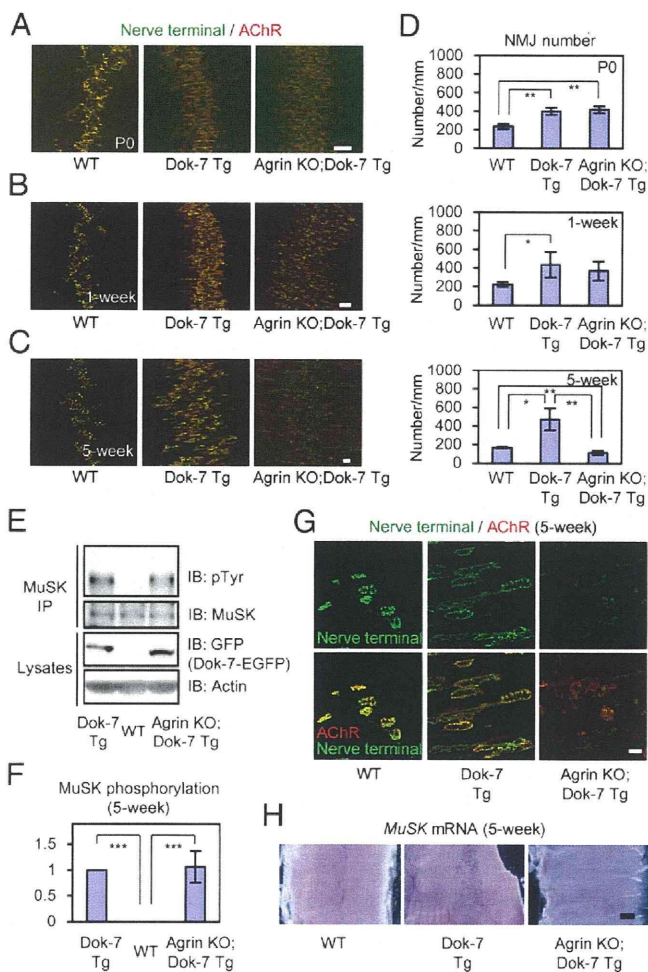


Fig. 5. Forced expression of Dok-7 maintains MuSK activation but not NMJs in agrin-deficient mice after birth. (A–C) Diaphragm muscles of WT, Dok-7 Tg, or Agrin KO; Dok-7 Tg mice at 0 (P0) (A), 1 (B), or 5 (C) weeks of age were stained with Btx (AChR) and antibodies to synapsin1 (“Nerve terminal”). (Scale bars, 100 μ m.) (D) The number of NMJs in diaphragm muscles was quantified. Error bars indicate mean \pm SD. Data were collected from three or more diaphragm muscles for each genotype. Asterisks denote significant statistical difference: * P < 0.05 and ** P < 0.01. (E) The limb-muscle lysates and anti-MuSK IP from the lysates of 5-wk-old mice were subjected to IB with the indicated antibodies. (F) Ratio of MuSK tyrosine phosphorylation to total MuSK was quantified. The relative intensity of MuSK phosphorylation in Dok-7 Tg was arbitrarily defined as 1. Error bars indicate mean \pm SD (n = 3). Asterisks denote significant statistical difference: *** P < 0.001. (G) Magnified views of NMJs in diaphragm muscles of 5-wk-old mice are shown. (Scale bars, 20 μ m.) (H) Diaphragm muscles of 5-wk-old mice were subjected to in situ hybridization with an antisense probe for *Musk*. (Scale bars, 500 μ m.)

Discussion

In the current study, we demonstrated that forced expression of Dok-7 in *Lrp4*-deficient embryos induced MuSK activation and restored muscle prepattern, showing that *Lrp4* is not required for MuSK activation by Dok-7 at least in these experimental settings (Figs. 3 and 4 and Fig. S2). However, MuSK was activated to a greater extent in Dok-7 Tg embryos than in those lacking *Lrp4*. These findings suggest that *Lrp4* facilitates Dok-7-mediated activation of MuSK, and thus at its normal expression levels Dok-7 needs *Lrp4* to adequately activate MuSK for induction of muscle prepattern. Therefore, interaction between *Lrp4* and MuSK might induce conformational change in MuSK to promote its susceptibility to Dok-7-mediated activation in vivo. Indeed, overexpression of *Lrp4* and MuSK in BaF3 or HEK293 cells induced partial activation of MuSK, and further stimulation with agrin led to higher MuSK activation (21, 22). Alternatively, but not mutually exclusively, the *Lrp4*-mediated partial activation of MuSK might induce a low level of phosphorylation of Tyr-553 that would stabilize binding of MuSK to Dok-7 via its phosphotyrosine-binding (PTB) domain and thus induce dimerization of the complex to facilitate further MuSK activation (30). However, we previously demonstrated that, in HEK293T cells, Dok-7 activates MuSK even in the presence of various types of mutations that disrupt their stable binding via the PTB domain and its target (17, 18). Therefore, further studies are required to determine whether the partial activation of MuSK by *Lrp4* observed in heterologous cells is relevant to the apparent cooperation between *Lrp4* and Dok-7 in MuSK activation in vivo.

Because agrin is secreted into the synaptic basal lamina and binds not only Lrp4, but also a variety of other NMJ proteins including laminins and dystroglycans (31), agrin could have roles other than activation of MuSK through such interactions. However, it was reported that modestly increased expression of MuSK in the skeletal muscle induces NMJ formation in agrin-deficient embryos, although highly increased expression induces postnatal lethality with abnormally scattered NMJ formation even in mice with intact agrin (29). These findings imply that, in the presence of Dok-7 and Lrp4, MuSK is activated as a result of increased expression to induce NMJ formation in agrin-deficient embryos, although MuSK activation per se was not examined in this study. In the current study, we demonstrate that forced expression of Dok-7 induced robust activation of MuSK and restored NMJ formation in agrin-deficient embryos (Figs. 1 and 2 and Fig. S1). These data together establish that MuSK activation can compensate for agrin deficiency in embryonic NMJ formation. In other words, agrin is required because Dok-7-mediated MuSK activation does not suffice for embryonic NMJ formation in the physiological setting. However, NMJs formed in agrin-deficient Dok-7 Tg embryos rapidly disappeared after birth (Fig. 5 *A–D*), and motor innervation and postsynaptic AChR clustering was impaired even in the remaining NMJs (Fig. 5*G* and Fig. 5*S8*). Given that the exogenous Dok-7-mediated MuSK activation was maintained at a high level (Fig. 5 *E* and *F* and Fig. 5*S7*), these findings indicate that agrin has a separate indispensable role as a synaptic organizer aside from MuSK activation for postnatal maintenance, but not embryonic formation, of NMJs. Uncovering the mechanisms by which agrin does this should illuminate why postnatal, but not prenatal, NMJs are vulnerable. This may also provide insight into CMS pathology because most CMSs show postnatal onset of muscle weakness as discussed further later.

Only a few elements that play indispensable roles in the postnatal maintenance, but not prenatal formation, of NMJs have been suggested (32). The laminin β 2-subunit is one such element; mice lacking it show no defects in NMJ formation during embryogenesis and the first few postnatal days, but develop presynaptic defects by 1 wk after birth, leading to lethality during the third postnatal week (33–35). Interestingly, agrin-deficient mice are rescued by muscle-specific expression of “mini-agrin,” which retains only agrin’s laminin-binding and MuSK-activating (Lrp4-binding) regions (36). Therefore, agrin may evoke signals other than MuSK activation by binding to laminins and/or Lrp4. Because the laminin β 2-subunit acts as an essential presynaptic organizer after, but not before, birth by binding to the presynaptic voltage-gated calcium channels at NMJs (33–35), agrin might promote the presynaptic specialization essential for NMJ maintenance via interaction with the laminins containing the β 2-subunit. Notably, this hypothetical role for agrin could explain our finding that agrin deficiency impaired motor innervation as judged by the coverage of presynaptic nerve terminals over postsynaptic AChR clusters (Fig. 5*G* and Fig. 5*S8B*), which implies a presynaptic defect. However, it remains unclear if the presynaptic defect is solely responsible for the postnatal loss of NMJs in Dok-7 Tg mice that lack agrin.

In agrin-deficient Dok-7 Tg mice, we also found that the loss of postnatal, but not prenatal, midmuscle restricted expression of the *MuSK* and *AChR α 1* transcripts (Fig. 5*H* and Fig. 5*S10*), which is important for the correct central localization of NMJs in skeletal muscle (2, 29). Although this transcriptional regulation is dependent on MuSK activity, these findings indicate that agrin plays an additional essential role distinct from MuSK activation in transcriptional regulation after, but not before, birth. Given that NMJs also disappeared after birth in agrin-deficient Dok-7 Tg mice, NMJs per se might be required for this midmuscle-restricted transcriptional regulation. However, this type of regulation occurs at E14.5 before NMJ formation and also occurs in the absence

of neuromuscular transmission resulting from a lack of ACh (37, 38). Therefore, agrin may play two distinct roles: one in the postnatal maintenance of NMJs and the other in postnatal midmuscle-restricted transcriptional regulation. Alternatively, NMJs could have an essential role aside from neuromuscular transmission in exerting such transcriptional regulation.

Interestingly, among agrin mutations found in patients with CMS, one mutation, V1727F, reduced agrin’s ability to activate MuSK in cultured myotubes (12), but another mutation, G1709R, showed no such reduction (13). However, injection of G1709R mutant agrin, but not the WT protein, into the skeletal muscle of 4-wk-old rats perturbed the organization of NMJs, implying that the G1709R mutation may impair agrin-mediated signaling to maintain postnatal NMJs without affecting its ability to activate MuSK. Similar disturbances in this agrin-mediated signaling pathway could also be involved in the pathogenesis of other types of CMSs with unknown etiology because CMSs frequently present with postnatal onset (39). Therefore, uncovering the role that agrin plays in the postnatal maintenance of NMJs, apart from its role in MuSK activation, would not only deepen our understanding of NMJs but also pave the way toward finding new therapeutic targets for CMSs.

Materials and Methods

Mouse Strains. The transgenic mice expressing Dok-7 tagged with EGFP (Dok-7-EGFP) under the control of the skeletal actin promoter and z-agrin-deficient or Lrp4-deficient (*Lrp4^{mut}*) mice were previously described (9, 19, 20). All experiments described here were approved by the Animal Care and Use Committee at the Institute of Medical Science, University of Tokyo.

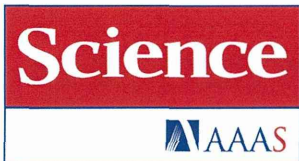
Immunoprecipitation and Immunoblotting. Tissue lysates were prepared from limb muscle with alkaline-lysis buffer (50 mM Tris-HCl, pH 9.5, 1 mM Na₃VO₄, 50 mM NaF, 1% sodium deoxycholate with a mixture of protease inhibitors). For immunoprecipitation, lysates were incubated with antibodies to MuSK (N-19 and C-19) or AChR β 1 (H-101) (Santa Cruz Biotechnology), followed by incubation with protein G-Sepharose (GE Healthcare). The immune complexes were washed four times and collected as immunoprecipitates. For immunoblotting, immunoprecipitates or tissue lysates were separated by SDS7.5% or 9% (wt/vol)-PAGE and transferred to a PVDF membrane (Millipore), which was then incubated with antibodies to phosphotyrosine (4G10) (Millipore), MuSK (AF562) (R&D Systems), AChR β 1 (H101), GFP (B-2), actin (I-19) (Santa Cruz Biotechnology), and Dok-7 (R&D Systems), washed, and incubated with horseradish peroxidase-labeled anti-mouse, anti-rabbit (GE Healthcare), anti-goat (Santa Cruz Biotechnology) IgG, or anti-rabbit light-chain antibodies (Jackson ImmunoResearch Laboratories). Band intensities were measured and analyzed using a LAS4000 imager with ImageQuant TL software (GE Healthcare). Data were assessed by paired or unpaired *t* test. The differences between samples with *P* values <0.05 were considered to be statistically significant.

Whole-Mount Tissue Staining and in Situ Hybridization. For whole-mount tissue staining, diaphragm muscles from mouse embryos at E14.5 or E18.5 and mice at 0 (P0), 1, or 5 wk of age were fixed in 1% paraformaldehyde in PBS for 2 h or overnight at 4 °C and then rinsed with PBS. After dissection of the connective tissue, the muscles were permeabilized with 1% Triton X-100 in PBS for 1 h and then incubated with rabbit antibodies against synaptophysin (Invitrogen) or synapsin1 (Cell Signaling) to label presynaptic nerve terminals and/or against neurofilament (Millipore) to label motor axons, followed by incubation with Alexa 647-conjugated anti-rabbit IgG and/or Alexa 594-conjugated α -bungarotoxin (Btx) (Invitrogen) to label postsynaptic AChR clusters. Confocal Z serial images were collected with a confocal laser-scanning microscope (FV1000, Olympus), collapsed into a single image, and analyzed with photoshop (Adobe) and cellSens (Olympus) software (19, 28, 29). Data were assessed by unpaired *t* test. The differences between samples with *P* values <0.05 were considered to be statistically significant. For in situ hybridization, diaphragm muscles dissected from mouse embryos at E18.5 or 5-wk-old mice were probed with a digoxigenin-labeled antisense riboprobe corresponding to mouse cDNA of *AChR α 1* or *MuSK*, and images were obtained using the stereo microscope SZX16 fitted with a DP-70 camera (Olympus) as described previously (19).

ACKNOWLEDGMENTS. We thank R. F. Whittier for critically reading the manuscript and for thoughtful discussions and M. Zenibayashi for animal care. This work was supported by Grants-in-Aid for Scientific Research

from the Ministry of Education, Culture, Sports, Science and Technology of Japan (to T.T. and Y.Y.) and by National Institutes of Health Grant NS054154 (to R.W.B.).

1. Sanes JR, Lichtman JW (2001) Induction, assembly, maturation and maintenance of a postsynaptic apparatus. *Nat Rev Neurosci* 2(11):791–805.
2. Burden SJ (2002) Building the vertebrate neuromuscular synapse. *J Neurobiol* 53(4):501–511.
3. Engel AG, Ohno K, Sine SM (2003) Sleuthing molecular targets for neurological diseases at the neuromuscular junction. *Nat Rev Neurosci* 4(5):339–352.
4. Vincent A, et al. (2003) Antibodies in myasthenia gravis and related disorders. *Ann N Y Acad Sci* 998:324–335.
5. DeChiara TM, et al. (1996) The receptor tyrosine kinase MuSK is required for neuromuscular junction formation in vivo. *Cell* 85(4):501–512.
6. Hesser BA, Henschel O, Witzemann V (2006) Synapse disassembly and formation of new synapses in postnatal muscle upon conditional inactivation of MuSK. *Mol Cell Neurosci* 31(3):470–480.
7. Chevessier F, et al. (2004) *MUSK*, a new target for mutations causing congenital myasthenic syndrome. *Hum Mol Genet* 13(24):3229–3240.
8. Gautam M, et al. (1996) Defective neuromuscular synaptogenesis in agrin-deficient mutant mice. *Cell* 85(4):525–535.
9. Burgess RW, Nguyen QT, Son YJ, Lichtman JW, Sanes JR (1999) Alternatively spliced isoforms of nerve- and muscle-derived agrin: Their roles at the neuromuscular junction. *Neuron* 23(1):33–44.
10. Bogdanik LP, Burgess RW (2011) A valid mouse model of *AGRIN*-associated congenital myasthenic syndrome. *Hum Mol Genet* 20(23):4617–4633.
11. Samuel MA, Valdez G, Tapia JC, Lichtman JW, Sanes JR (2012) Agrin and synaptic laminin are required to maintain adult neuromuscular junctions. *PLoS ONE* 7(10):e46663.
12. Maselli RA, et al. (2012) LG2 agrin mutation causing severe congenital myasthenic syndrome mimics functional characteristics of non-neural (α -) agrin. *Hum Genet* 131(7):1123–1135.
13. Huzé C, et al. (2009) Identification of an agrin mutation that causes congenital myasthenia and affects synapse function. *Am J Hum Genet* 85(2):155–167.
14. Lin W, et al. (2001) Distinct roles of nerve and muscle in postsynaptic differentiation of the neuromuscular synapse. *Nature* 410(6832):1057–1064.
15. Misgeld T, Kummer TT, Lichtman JW, Sanes JR (2005) Agrin promotes synaptic differentiation by counteracting an inhibitory effect of neurotransmitter. *Proc Natl Acad Sci USA* 102(31):11088–11093.
16. Lin W, et al. (2005) Neurotransmitter acetylcholine negatively regulates neuromuscular synapse formation by a Cdk5-dependent mechanism. *Neuron* 46(4):569–579.
17. Okada K, et al. (2006) The muscle protein Dok-7 is essential for neuromuscular synaptogenesis. *Science* 312(5781):1802–1805.
18. Hamuro J, et al. (2008) Mutations causing *DOK7* congenital myasthenia ablate functional motifs in Dok-7. *J Biol Chem* 283(9):5518–5524.
19. Inoue A, et al. (2009) Dok-7 activates the muscle receptor kinase MuSK and shapes synapse formation. *Sci Signal* 2(59):ra7.
20. Weatherbee SD, Anderson KV, Niswander LA (2006) LDL-receptor-related protein 4 is crucial for formation of the neuromuscular junction. *Development* 133(24):4993–5000.
21. Kim N, et al. (2008) Lrp4 is a receptor for Agrin and forms a complex with MuSK. *Cell* 135(2):334–342.
22. Zhang B, et al. (2008) LRP4 serves as a coreceptor of agrin. *Neuron* 60(2):285–297.
23. Yamanashi Y, Higuchi O, Beeson D (2008) Dok-7/MuSK signaling and a congenital myasthenic syndrome. *Acta Myol* 27:25–29.
24. Beeson D, et al. (2006) Dok-7 mutations underlie a neuromuscular junction synaptopathy. *Science* 313(5795):1975–1978.
25. Herbst R, Avetisova E, Burden SJ (2002) Restoration of synapse formation in Musk mutant mice expressing a Musk/Trk chimeric receptor. *Development* 129(23):5449–5460.
26. Fuhrer C, Sugiyama JE, Taylor RG, Hall ZW (1997) Association of muscle-specific kinase MuSK with the acetylcholine receptor in mammalian muscle. *EMBO J* 16(11):4951–4960.
27. Yumoto N, Kim N, Burden SJ (2012) Lrp4 is a retrograde signal for presynaptic differentiation at neuromuscular synapses. *Nature* 489(7416):438–442.
28. Wu H, et al. (2012) Distinct roles of muscle and motoneuron LRP4 in neuromuscular junction formation. *Neuron* 75(1):94–107.
29. Kim N, Burden SJ (2008) MuSK controls where motor axons grow and form synapses. *Nat Neurosci* 11(1):19–27.
30. Bergamin E, Hallock PT, Burden SJ, Hubbard SR (2010) The cytoplasmic adaptor protein Dok7 activates the receptor tyrosine kinase MuSK via dimerization. *Mol Cell* 39(1):100–109.
31. Singhal N, Martin PT (2011) Role of extracellular matrix proteins and their receptors in the development of the vertebrate neuromuscular junction. *Dev Neurobiol* 71(11):982–1005.
32. Wu H, Xiong WC, Mei L (2010) To build a synapse: Signaling pathways in neuromuscular junction assembly. *Development* 137(7):1017–1033.
33. Noakes PG, Gautam M, Mudd J, Sanes JR, Merlie JP (1995) Aberrant differentiation of neuromuscular junctions in mice lacking α -laminin/laminin β 2. *Nature* 374(6519):258–262.
34. Nishimune H, Sanes JR, Carlson SS (2004) A synaptic laminin-calcium channel interaction organizes active zones in motor nerve terminals. *Nature* 432(7017):580–587.
35. Fox MA, et al. (2007) Distinct target-derived signals organize formation, maturation, and maintenance of motor nerve terminals. *Cell* 129(1):179–193.
36. Lin S, et al. (2008) Muscle-wide secretion of a miniaturized form of neural agrin rescues focal neuromuscular innervation in agrin mutant mice. *Proc Natl Acad Sci USA* 105(32):11406–11411.
37. Misgeld T, et al. (2002) Roles of neurotransmitter in synapse formation: Development of neuromuscular junctions lacking choline acetyltransferase. *Neuron* 36(4):635–648.
38. Brandon EP, et al. (2003) Aberrant patterning of neuromuscular synapses in choline acetyltransferase-deficient mice. *J Neurosci* 23(2):539–549.
39. Abicht A, et al. (2012) Congenital myasthenic syndromes: Achievements and limitations of phenotype-guided gene-after-gene sequencing in diagnostic practice: a study of 680 patients. *Hum Mutat* 33(10):1474–1484.



***DOK7* gene therapy benefits mouse models of diseases characterized by defects in the neuromuscular junction**

Sumimasa Arimura *et al.*
Science **345**, 1505 (2014);
DOI: 10.1126/science.1250744

This copy is for your personal, non-commercial use only.

If you wish to distribute this article to others, you can order high-quality copies for your colleagues, clients, or customers by [clicking here](#).

Permission to republish or repurpose articles or portions of articles can be obtained by following the guidelines [here](#).

The following resources related to this article are available online at www.sciencemag.org (this information is current as of September 18, 2014):

Updated information and services, including high-resolution figures, can be found in the online version of this article at:
<http://www.sciencemag.org/content/345/6203/1505.full.html>

Supporting Online Material can be found at:
<http://www.sciencemag.org/content/suppl/2014/09/17/345.6203.1505.DC1.html>

This article **cites 43 articles**, 19 of which can be accessed free:
<http://www.sciencemag.org/content/345/6203/1505.full.html#ref-list-1>

This article appears in the following **subject collections**:
Medicine, Diseases
<http://www.sciencemag.org/cgi/collection/medicine>

29. A. Timmer, R. J. Hilsden, J. Cole, D. Hailey, L. R. Sutherland. *BMC Med. Res. Methodol.* **2**, 7 (2002).
30. K. P. Lee, E. A. Boyd, J. M. Holroyd-Leduc, P. Bacchetti, L. A. Bero. *Med. J. Aust.* **184**, 621–626 (2006).
31. K. Okike, M. S. Kocher, C. T. Mehlman, J. D. Heckman, M. Bhandari. *J. Bone Joint Surg.* **90**, 595–601 (2008).
32. K. Dickersin, S. Chan, T. C. Chalmers, H. S. Sacks, H. Smith Jr., *Control. Clin. Trials* **8**, 343–353 (1987).
33. K. Dickersin, Y. I. Min, C. L. Meinert. *JAMA* **267**, 374–378 (1992).
34. K. Dickersin, Y. I. Min. *Online J. Curr. Clin. Trials* **1993**, 50 (1993).
35. R. M. D. Smyth et al., *BMJ* **342** (jan06 1), c7153 (2011).
36. H. Cooper, K. DeNeve, K. Charlton. *Psychol. Methods* **2**, 447–452 (1997).
37. G. V. B. Glass, B. McGaw, M. L. Smith. *Meta Analysis in Social Research* (Sage, Beverly Hills, CA, 1981).
38. The rate at which research-initiated proposals are approved by the peer reviewers engaged by TESS is provided in the supplementary materials.
39. TESS archive: www.tessexperiments.org.
40. Materials and methods are available as supplementary materials on Science Online.
41. K. Casey, R. Glenmerster, E. Miguel, Q. J. Econ. **127**, 1755–1812 (2012).

ACKNOWLEDGMENTS

Data and replication code are available on GitHub (DOI: 10.5281/zenodo.11300). All authors contributed equally to all aspects of the research. No funding was required for this article. The authors declare no conflicts of interest. We thank seminar participants at the 2014 Annual Meeting of the Midwest Political Science Association, the 2014 Annual Meeting of the Society for

Political Methodology, the 2014 West Coast Experiments Conference, Stanford University, and University of California, San Diego. We thank C. McConnell and S. Liu for valuable research assistance.

SUPPLEMENTARY MATERIALS

www.sciencemag.org/content/345/6203/1502/suppl/DC1
Materials and Methods
Supplementary Text
Fig. S1
Tables S1 to S7
Reference (42)

1 May 2014; accepted 14 August 2014
Published online 28 August 2014;
10.1126/science.1255484

NEUROMUSCULAR DISEASE

DOK7 gene therapy benefits mouse models of diseases characterized by defects in the neuromuscular junction

Sumimasa Arimura,¹ Takashi Okada,² Tohru Tezuka,¹ Tomoko Chiyo,² Yuko Kasahara,² Toshiro Yoshimura,³ Masakatsu Motomura,⁴ Nobuaki Yoshida,⁵ David Beeson,⁶ Shin'ichi Takeda,² Yuji Yamanashi^{1*}

The neuromuscular junction (NMJ) is the synapse between a motor neuron and skeletal muscle. Defects in NMJ transmission cause muscle weakness, termed myasthenia. The muscle protein Dok-7 is essential for activation of the receptor kinase MuSK, which governs NMJ formation, and *DOK7* mutations underlie familial limb-girdle myasthenia (*DOK7* myasthenia), a neuromuscular disease characterized by small NMJs. Here, we show in a mouse model of *DOK7* myasthenia that therapeutic administration of an adeno-associated virus (AAV) vector encoding the human *DOK7* gene resulted in an enlargement of NMJs and substantial increases in muscle strength and life span. When applied to model mice of another neuromuscular disorder, autosomal dominant Emery-Dreifuss muscular dystrophy, *DOK7* gene therapy likewise resulted in enlargement of NMJs as well as positive effects on motor activity and life span. These results suggest that therapies aimed at enlarging the NMJ may be useful for a range of neuromuscular disorders.

The neurotransmitter acetylcholine (ACh) is released from the presynaptic motor nerve terminal and binds to ACh receptors (AChRs) on the postsynaptic muscle membrane of the neuromuscular junction (NMJ), which forms in the central region of each myotube (1, 2). To achieve efficient neuromuscular transmission, AChRs must be densely clustered on the postsynaptic membrane (1, 2). Impaired AChR clustering is associated with disorders of neuromuscular

transmission, including subtypes of congenital myasthenic syndromes and myasthenia gravis (2–4). The muscle-specific receptor tyrosine kinase MuSK is required for the formation and maintenance of NMJs (1, 2).

The cytoplasmic protein Dok-7 (downstream of tyrosine kinases 7) is an essential activator of the receptor kinase MuSK, and mice lacking Dok-7 form no NMJs (5–8). Recessive loss- or reduction-of-function mutations in the human *DOK7* gene underlie a limb-girdle type of congenital myasthenic syndrome, *DOK7* myasthenia, a disorder characterized by NMJs that are about half the normal size (7, 9, 10). In contrast to many NMJ channelopathies (11), *DOK7* myasthenia is not associated with abnormalities in the function and local density of AChRs or the quantal release per unit size of the endplates (the region of synaptic specialization on the myotube). These observations suggest that *DOK7* myasthenia should be classified as a synaptopathy rather than a channelopathy (2, 7). Interestingly, there is ac-

cumulating evidence that NMJ structural defects may be a common feature of other neuromuscular disorders (12–18), including muscular dystrophy (MD), amyotrophic lateral sclerosis (ALS), spinal muscular atrophy (SMA), and age-related muscle weakness or sarcopenia. Indeed, studies of patients with autosomal dominant Emery-Dreifuss muscular dystrophy (AD-EDMD) and a mouse model of this disease have produced data suggestive of inefficient neuromuscular transmission (12). Because the size of NMJs is an important determinant of NMJ function (2), these observations raise the possibility that enlargement of the synaptic area may mitigate muscle weakness associated with defective NMJ structure.

We previously generated Dok-7 transgenic (Tg) mice that overexpress Dok-7 uniformly throughout the skeletal muscle under the control of the human skeletal α -actin (HSA) promoter (6). Using these mice, we found that forced expression of Dok-7 in vivo enhanced the activation of muscle-specific kinase MuSK and subsequent NMJ formation at the correct, central region of muscle fibers in embryos (6). Consistent with this, Dok-7 Tg mice showed greatly enlarged NMJs at 12 weeks of age (fig. S1A). Because exogenous Dok-7 was expressed only in the skeletal muscle (6), these data indicate that forced expression of Dok-7 in muscle triggers not only intramuscular signaling but also retrograde signaling that enlarges motor axon terminals. Interestingly, although these mice have enlarged NMJs, they did not exhibit obvious defects in motor activity, as determined by wire-hang and rotarod tests (fig. S1, B and C). Together, these findings suggest that Dok-7-mediated enhancement of NMJ formation merits investigation as a possible therapeutic approach for neuromuscular disorders associated with an NMJ synaptopathy.

To facilitate Dok-7-mediated NMJ formation in the muscle, we generated AAV-D7, a recombinant adeno-associated virus (AAV) serotype 9 (AAV9) vector carrying the human *DOK7* gene tagged with enhanced green fluorescent protein (EGFP) under the control of the cytomegalovirus (CMV) promoter. This promoter shows higher activity in skeletal muscle than the HSA promoter (19). The AAV vector is a powerful tool for delivering therapeutic genes to skeletal muscle and other tissues (20, 21). We first treated C2C12 myotubes

¹Division of Genetics, The Institute of Medical Science, The University of Tokyo, Tokyo, Japan. ²Department of Molecular Therapy, National Institute of Neuroscience, National Center of Neurology and Psychiatry, Tokyo, Japan. ³Department of Occupational Therapy, Nagasaki University School of Health Sciences, Nagasaki, Japan. ⁴Department of Electrical and Electronics Engineering, Faculty of Engineering, Nagasaki Institute of Applied Science, Nagasaki, Japan. ⁵Laboratory of Developmental Genetics, The Institute of Medical Science, The University of Tokyo, Tokyo, Japan. ⁶Neurosciences Group, Weatherall Institute of Molecular Medicine, University of Oxford, Oxford, UK.

*Corresponding author. E-mail: yamanashi@ims.u-tokyo.ac.jp

with AAV-D7 and observed an increase in the number of AChR clusters (fig. S2), as expected from previous work (5, 7, 9). We next treated 8-week-old wild-type (WT) mice with 4.0×10^{11} viral genomes (vg) of AAV-D7, delivered by a single intravenous injection, and compared them with control, untreated mice. One week after the injection, NMJs were clearly enlarged in the central region of the diaphragm muscle of AAV-D7-treated mice, with exogenous expression of Dok-7 throughout the myotubes (fig. S3 and Fig. 1, A and B). MuSK activation was augmented in the muscle as judged by elevated phosphorylation of MuSK and AChR, the latter known to be dependent on MuSK activation (Fig. 1, C and D). These results demonstrate that forced expression of Dok-7 in adult mice promotes MuSK-mediated formation of NMJs, leading to their enlargement within a week of AAV-D7 treatment. WT mice treated with AAV-D7 did not show any abnormalities in motor activity, as determined by grip strength, wire-hang, and rotarod tests (fig. S4), or in histology of the skeletal muscle, heart, and liver, which are the major target tissues of this AAV9 vector in mice (fig. S5) (22). We confirmed exogenous expression of Dok-7 in the heart (fig. S6) and in skeletal muscle (fig. S3 and Fig. 1A) after AAV-D7 treatment.

To investigate whether forced expression of Dok-7 and subsequent enlargement of NMJs in vivo mitigates disease progression after onset of *DOK7* myasthenia, we generated Dok-7 knock-in (KI) mice homozygous for the frameshift mutation (c.1124_1127dupTGCC), which corresponds to the most prevalent mutation in patients (fig. S7) (7, 10, 23–25). Dok-7^{+KI} and littermate WT mice displayed no obvious abnormal phenotype. By contrast, Dok-7^{KI/KI} mice (Dok-7 KI mice) exhibited characteristic features of severe muscle weakness: These mice died between postnatal day 13 (P13) and P20, exhibited about 25% of the body weight of WT mice at P12, and developed apparent disturbance in gait by P9 (fig. S8). Unlike Dok-7^{+KI} and littermate WT mice, Dok-7 KI mice were too weak for the measurement of muscle strength. Furthermore, they showed abnormally small NMJs lacking postsynaptic folding (figs. S9 and S10), a pathological feature seen in patients with *DOK7* myasthenia (26). The c.1124_1127dupTGCC mutation is a reduction-of-function mutation in terms of MuSK activation in C2C12 myotubes (7, 9). Consistent with this, Dok-7 KI mice exhibited decreased MuSK activity in skeletal muscle, as judged by attenuated phosphorylation of AChR and MuSK (fig. S11) (see below). Thus, the Dok-7 KI mice develop defects similar to those found in patients with *DOK7* myasthenia, although the mice (hereafter referred to as “*DOK7* myasthenia mice”) exhibit a more severe phenotype.

To determine whether *DOK7* gene therapy provides beneficial effects to *DOK7* myasthenia mice, we administered 2.0×10^{11} vg of AAV-D7 by intraperitoneal injection to the animals at P9 to P12. At P9, these mice required at least 10 s to right themselves after being placed on their side, confirming disease onset. A single-dose treatment with AAV-D7 led to marked recovery of the *DOK7*

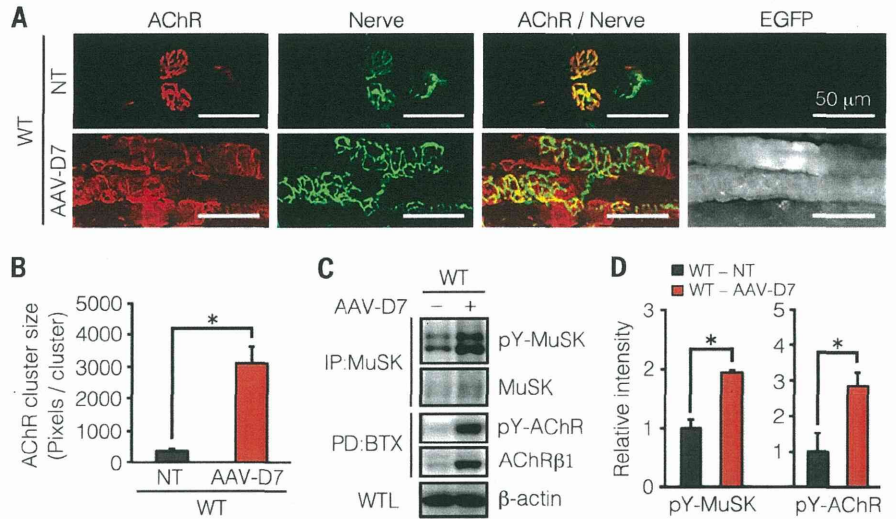


Fig. 1. AAV-D7 treatment promotes MuSK-mediated NMJ formation. WT mice were treated or untreated with 4.0×10^{11} vg of AAV-D7 at P56 and subjected to the following assays at P63. **(A)** Whole-mount staining of NMJs on the diaphragm muscle. Axons and nerve terminals (green) were stained with antibodies to neurofilament and synaptophysin, and AChRs (red) were labeled with α -bungarotoxin (BTX). Expression of Dok-7 tagged with EGFP (gray) was monitored by EGFP. NT, not treated. **(B)** Quantified data for the size of each AChR cluster in the diaphragm muscle ($n = 30$ microscopic fields in 6 mice; male = 3, female = 3). **(C)** Immunoblotting for tyrosine phosphorylation of MuSK or AChR and for β -actin in the hind-limb muscle. MuSK immunoprecipitates (IP) from whole-tissue lysates (WTL) of the hind-limb muscle were subjected to immunoblotting for phosphotyrosine (pY) and MuSK. AChRs pulled down with BTX-Sepharose (PD) from WTL were subjected to immunoblotting for pY or the $\beta 1$ subunit of AChR. **(D)** Quantified data for tyrosine phosphorylation of MuSK and AChR in the hind-limb muscle ($n = 3$ mice; male = 1 to 2, female = 1 to 2). Values in (B) and (D) are means \pm SD. * $P < 0.05$ by Student's *t* test.

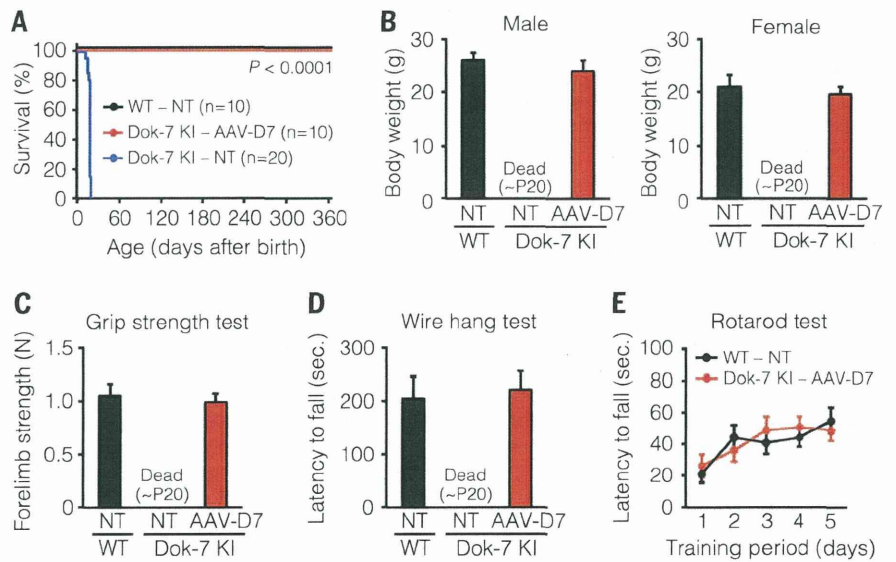


Fig. 2. Dok-7 therapy restores motor activity and survival of *DOK7* myasthenia mice. Mice were treated or untreated with 2.0×10^{11} vg of AAV-D7 at P9 to P12. **(A)** Kaplan-Meier survival curves of WT littermates and Dok-7 KI mice (*DOK7* myasthenia mice) ($n = 10$ to 20 mice; male = 4 to 10, female = 6 to 10). NT, not treated. **(B)** Body weight at P56 ($n = 4$ to 6 mice; male = 5, female = 4 to 6). **(C to E)** Motor activity at P56 determined by (C) grip strength, (D) wire-hang, and (E) rotarod tests ($n = 10$ mice; male = 4 to 5, female = 5 to 6). P value (A) was calculated by log-rank test (Dok-7 KI – NT versus Dok-7 KI – AAV-D7). Values in (B) to (E) are means \pm SD.

myasthenia mice. All AAV-D7-treated mice survived for at least 1 year with no apparent abnormality, whereas all untreated and AAV-EGFP-treated

control mice died by P20 (Fig. 2A and fig. S12). Indeed, body weight and motor activity—as determined by grip strength, wire-hang, and rotarod

tests—of AAV-D7-treated mice approximated those of age-matched WT controls by P56 (Fig. 2, B to E). Similarly, forced expression of a *DOK7* transgene

Fig. 3. Dok-7 therapy promotes MuSK-mediated NMJ formation in *DOK7* myasthenia mice. Mice were treated or untreated with 2.0×10^{11} vg of AAV-D7 at P9 and subjected to the following assays at P14. **(A)** Immunoblotting for tyrosine phosphorylation of MuSK or AChR and for β -actin in the hind-limb muscle. Experiments were performed as in Fig. 1C. **(B)** Quantified data for tyrosine phosphorylation of MuSK and AChR in the hind-limb muscle ($n = 3$ mice; male = 1 to 2, female = 1 to 2). **(C)** Whole-mount staining of NMJs on the diaphragm muscle. Axons and nerve terminals (green), AChRs (red), and Dok-7 tagged with EGFP (gray) were visualized as in Fig. 1A. **(D)** Quantified data for the size of each AChR cluster in the diaphragm muscle ($n = 30$ microscopic fields in 6 mice; male = 3, female = 3). Values in (B) and (D) are means \pm SD. * $P < 0.05$ by analysis of variance (ANOVA) and Dunnett's test.

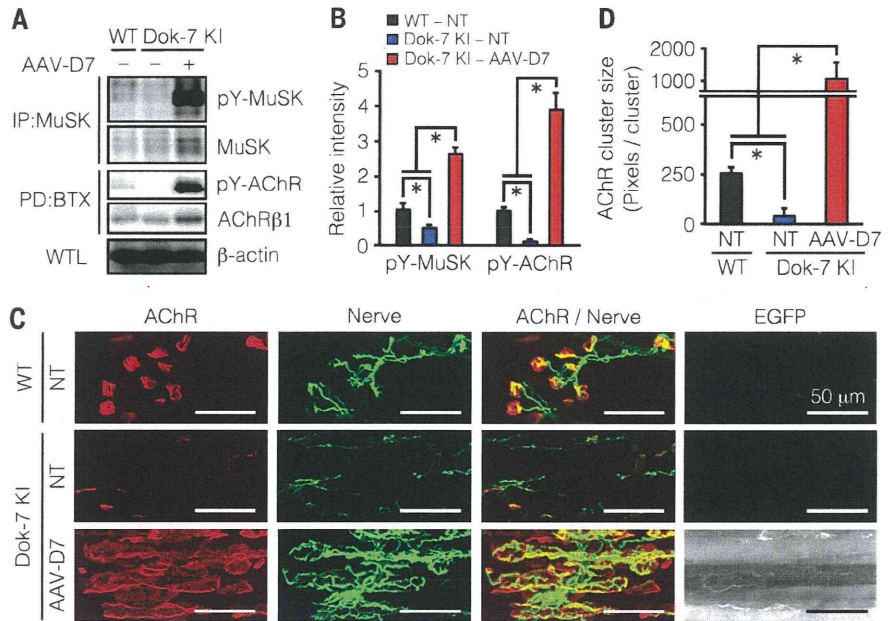
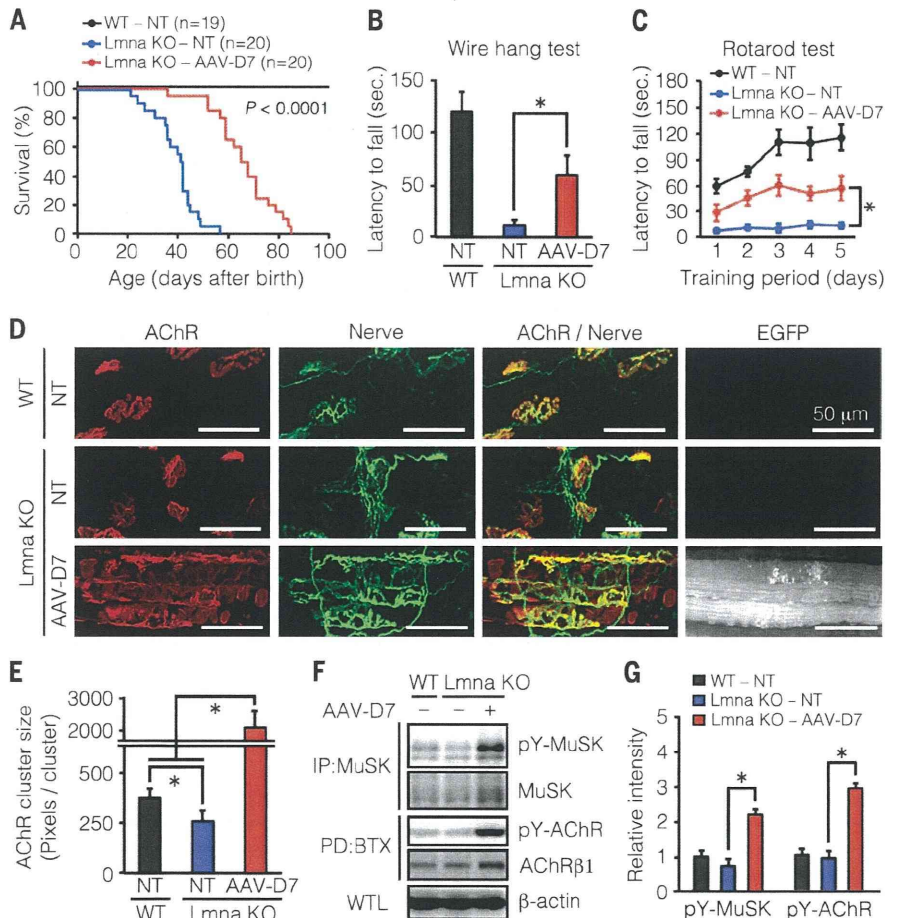


Fig. 4. The effect of Dok-7 therapy in a mouse model of AD-EDMD. Mice were treated or untreated with 4.0×10^{11} vg of AAV-D7 at P16 and subjected to the following assays. **(A)** Kaplan-Meier survival curves of WT littermates and *Lmna* KO mice (AD-EDMD mice) ($n = 19$ to 20 mice; male = 9 to 12, female = 8 to 11). NT, not treated. **(B)** Motor activity at P35, determined by (B) wire-hang and (C) rotarod tests ($n = 8$ to 10 mice; male = 4 to 6, female = 4 to 5). **(D)** Whole-mount staining of NMJs on the diaphragm muscle at P42. Axons and nerve terminals (green), AChRs (red), and Dok-7 tagged with EGFP (gray) were visualized as in Fig. 1A. **(E)** Quantified data for the size of each AChR cluster in the diaphragm muscle at P42 ($n = 30$ microscopic fields in 6 mice; male = 3 to 4, female = 2 to 3). **(F)** Immunoblotting for tyrosine phosphorylation of MuSK or AChR and for β -actin in the hind-limb muscle at P42. Experiments were performed as in Fig. 1C. **(G)** Quantified data for tyrosine phosphorylation of MuSK and AChR in the hind-limb muscle at P42 ($n = 3$ mice; male = 1 to 2, female = 1 to 2). P value (A) was calculated by log-rank test (*Lmna* KO - NT versus *Lmna* KO - AAV-D7). Values in (B), (C), (E), and (G) are means \pm SD. * $P < 0.05$ by analysis of variance (ANOVA) and Dunnett's test.



specifically in skeletal muscle restored survival and motor activity of *DOK7* myasthenia mice as determined by wire-hang and rotarod tests, indicating that muscle-specific expression of Dok-7 is sufficient to rescue these mice (fig. S13, A to C).

We next investigated whether AAV-D7 treatment promotes activation of MuSK and subsequent enlargement of NMJs in *DOK7* myasthenia mice. We found that MuSK and AChR phosphorylation was strongly elevated in *DOK7* myasthenia mice just 5 days after treatment with AAV-D7 (Fig. 3, A and B). Consistent with this, NMJs were greatly enlarged in *DOK7* myasthenia mice within 5 days of treatment (Fig. 3, C and D, and fig. S14) and remained enlarged at 8 weeks of age (fig. S15). Together, these data demonstrate that treatment with AAV-D7 (hereafter referred to as “Dok-7 therapy”) facilitates MuSK-mediated NMJ formation, resulting in stable enlargement of NMJs, restoration of motor activity, and enhanced survival of *DOK7* myasthenia mice.

Because AAV-D7 enlarges NMJs not only in *DOK7* myasthenia mice but also in WT mice, we hypothesized that Dok-7 therapy might be applicable to other types of neuromuscular disorders that are associated with abnormalities of NMJ structure but not caused by *DOK7* mutations. As noted above, AD-EDMD is one such candidate. AD-EDMD is caused by mutations in the *LMNA* gene, which encodes lamin A/C, an important determinant of interphase nuclear architecture (27). Patients with AD-EDMD develop cardiac defects and skeletal muscle weakness (28). Although pacemaker and implantable cardioverter defibrillator (ICD) insertion helps address the cardiac defects (29), there is no effective treatment for skeletal muscle weakness. Histology and gene expression profiles of muscle biopsies from patients with AD-EDMD are suggestive of alterations in NMJ structure (12, 30, 31).

We studied a mouse model of AD-EDMD (hereafter referred to as “AD-EDMD mice”) that is genetically deficient in lamin A/C and that has structurally abnormal and functionally inefficient NMJs (12, 30). At P16, we administered 4.0×10^{11} vg of AAV-D7 into the AD-EDMD mice by a single intraperitoneal injection. Disease onset was confirmed in each AD-EDMD mouse at P16, when the animals showed hind-limb paralysis and required at least 10 s to right themselves after being placed on their sides. We found that Dok-7 therapy prolonged survival of AD-EDMD mice (Fig. 4A). Mice receiving Dok-7 therapy, but not those receiving AAV-EGFP treatment, lived an average of 29 days longer than untreated mice ($P < 0.0001$, log-rank test) (Fig. 4A and fig. S16). In addition, Dok-7 therapy increased latency to fall of AD-EDMD mice, as determined by wire-hang and rotarod tests by 49 s and 44 s, respectively, over untreated mice ($P < 0.05$, Dunnett’s test) (Fig. 4, B and C), indicating enhanced motor activity. Forced expression of Dok-7 specifically in skeletal muscle via a transgene also enhanced AD-EDMD mouse survival and motor activity, as determined by wire-hang and rotarod tests, indicating that muscle-specific expression of Dok-7 is sufficient to benefit these mice (fig. S13, D to F).

Dok-7 therapy enhanced MuSK activation and enlarged NMJs in the skeletal muscle within 26 days of treatment (Fig. 4, D to G), and the NMJs in control, untreated AD-EDMD mice were significantly smaller than those in WT mice (Fig. 4, D and E). Electrocardiographic and histological analyses showed that Dok-7 therapy did not benefit heart function in AD-EDMD mice (fig. S17). It is possible that the beneficial effects of Dok-7 therapy on muscle weakness are partially masked in these mice by heart failure, which, as noted above, would be treatable in patients with AD-EDMD by pacemaker and ICD insertion (29). These findings suggest that Dok-7 therapy might be beneficial for patients with AD-EDMD.

The mechanisms through which Dok-7 therapy alleviates muscle weakness in mouse models of *DOK7* myasthenia and AD-EDMD remain to be determined. We speculate that, in addition to an effect on the postsynaptic region of muscle, the mechanism likely involves retrograde signaling from the muscle to the nerve. This idea is consistent with the observation that enlargement of the nerve terminals at NMJs is seen in the Dok-7 Tg mice that overexpress Dok-7 only in the skeletal muscle, as well as in AAV-D7-treated mice.

Recent studies of mouse models of ALS and SMA revealed that peripheral motor nerve degeneration first manifests as reduction of the nerve terminal area with subsequent denervation at NMJs, and then proceeds proximally, a pattern known as “dying-back” pathology (32, 33). Consistent with this, autopsies of patients with ALS or SMA suggest that motor neuron pathology begins at the distal axon and proceeds proximally (32, 34). Because AAV-D7 has the potential to enlarge the nerve terminals at NMJs, it is tempting to speculate that Dok-7 therapy may counteract the “dying-back” pathology at NMJs and be beneficial in these multifactorial disorders of mostly unknown etiology. Interestingly, in a recent study of the SOD1 (superoxide dismutase 1) G93A Tg mouse model of ALS, it was reported that a modest, muscle-specific increase in MuSK expression via a transgene delayed denervation at NMJs and improved motor activity, but not survival, of the mice (35). However, a previous study had shown that higher-level expression of MuSK in the muscle induces scattered NMJ formation throughout myotubes, leading to severe muscle weakness and ultimately to death (36). Dok-7 gene therapy may be a safer approach because it greatly facilitates correct, centrally localized NMJ enlargement without lethal effects for more than 1 year in *DOK7* myasthenia mice (Figs. 2A and 3C and figs. S14 and S15).

AAV-mediated gene transfer to skeletal muscle can result in long-term expression of the therapeutic gene. For instance, in a patient with hemophilia B, AAV-mediated expression of factor IX was detected even 10 years after a single intramuscular injection (37). In addition, although AAV capsid, rather than transgene, is the antigen that is targeted by the host immune responses in humans, this process can be controlled by a short course of treatment with immunosuppressant without loss of transgene expression (38), raising

prospects for long-term use of these vectors in therapies.

Our findings demonstrate that elevated Dok-7 expression, or any equivalent method that stably and safely enlarges the NMJ, has potential as a therapy for a variety of neuromuscular disorders that feature defects in NMJ structure, including those of unknown etiology. Such NMJ-targeted therapies could be administered alone or in combination with other therapies.

REFERENCES AND NOTES

1. S. J. Burden, *Genes Dev.* **12**, 133–148 (1998).
2. C. R. Slater, *Handb. Clin. Neurol.* **91**, 27–101 (2008).
3. A. G. Engel, K. Ohno, S. M. Sine, *Nat. Rev. Neurosci.* **4**, 339–352 (2003).
4. P. Cavalante, P. Bernasconi, R. Mantegazza, *Curr. Opin. Neurol.* **25**, 621–629 (2012).
5. K. Okada et al., *Science* **312**, 1802–1805 (2006).
6. A. Inoue et al., *Sci. Signal.* **2**, ra7 (2009).
7. D. Beeson et al., *Science* **313**, 1975–1978 (2006).
8. Y. Yamashita, T. Tezuka, K. Yokoyama, *J. Biochem.* **151**, 353–359 (2012).
9. J. Hamuro et al., *J. Biol. Chem.* **283**, 5518–5524 (2008).
10. D. Selcen et al., *Ann. Neurol.* **64**, 71–87 (2008).
11. G. G. Cellesia, *Clin. Neurophysiol.* **112**, 2–18 (2001).
12. A. Méjat et al., *J. Cell Biol.* **184**, 31–44 (2009).
13. P. C. Ghedini et al., *Muscle Nerve* **38**, 1585–1594 (2008).
14. J. D. Gumerson et al., *Hum. Mol. Genet.* **22**, 757–768 (2013).
15. F. Saito et al., *J. Neurochem.* **101**, 1712–1722 (2007).
16. L. R. Fischer et al., *Exp. Neurol.* **185**, 232–240 (2004).
17. S. Kariya et al., *Hum. Mol. Genet.* **17**, 2552–2569 (2008).
18. Y. C. Jang, H. Van Remmen, *Exp. Gerontol.* **46**, 193–198 (2011).
19. J. N. Hagstrom et al., *Blood* **95**, 2536–2542 (2000).
20. M. Nonnenmacher, T. Weber, *Gene Ther.* **19**, 649–658 (2012).
21. F. Mingozzi, K. A. High, *Nat. Rev. Genet.* **12**, 341–355 (2011).
22. C. Zincarelli, S. Soltys, G. Rengo, J. E. Rabinowitz, *Mol. Ther.* **16**, 1073–1080 (2008).
23. J. S. Müller et al., *Brain* **130**, 1497–1506 (2007).
24. J. Palace et al., *Brain* **130**, 1507–1515 (2007).
25. M. Srour et al., *Neuromuscul. Disord.* **20**, 453–457 (2010).
26. C. R. Slater et al., *Brain* **129**, 2061–2076 (2006).
27. B. Burke, C. L. Stewart, *Annu. Rev. Genomics Hum. Genet.* **7**, 369–405 (2006).
28. H. J. Worman, G. Bonne, *Exp. Cell Res.* **313**, 2121–2133 (2007).
29. C. Meune et al., *N. Engl. J. Med.* **354**, 209–210 (2006).
30. T. Sullivan et al., *J. Cell Biol.* **147**, 913–920 (1999).
31. F. J. Ramos et al., *Sci. Transl. Med.* **4**, 144ra103 (2012).
32. L. M. Murray, K. Talbot, T. H. Gillingswater, *Neuropathol. Appl. Neurobiol.* **36**, 133–156 (2010).
33. C. Cifuentes-Diaz et al., *Hum. Mol. Genet.* **11**, 1439–1447 (2002).
34. G. Bruneteau et al., *Brain* **136**, 2359–2368 (2013).
35. M. J. Pérez-García, S. J. Burden, *Cell Reports* **2**, 497–502 (2012).
36. N. Kim, S. J. Burden, *Nat. Neurosci.* **11**, 19–27 (2008).
37. G. Buchlis et al., *Blood* **119**, 3038–3041 (2012).
38. A. C. Nathwani et al., *N. Engl. J. Med.* **365**, 2357–2365 (2011).

ACKNOWLEDGMENTS

We are grateful to C. L. Stewart and Y. Hayashi for the *Lmna* knock-out (KO) mice (AD-EDMD mice) and to J. M. Wilson for the helper plasmid pRep2Cap9. We thank R. F. Whittier and S. Miyoshi for critical reading of the manuscript. This work was supported by Grants-in-Aid of Scientific Research and of the Translational Research Network Program from the Ministry of Education, Culture, Sports, Science, and Technology of Japan. Y.Y. is an inventor on a patent (Japan patent P5339246 and U.S. patent 8222383) that covers the use of human *DOK7* cDNA for commercial purposes. University of Pennsylvania holds a patent (Japan patent P5054975 and U.S. patent 7906111) that covers the use of AAV9 for commercial purposes.

SUPPLEMENTARY MATERIALS

www.sciencemag.org/content/345/6203/1505/suppl/DC1
Materials and Methods
Figs. S1 to S17
Reference (39–43)

13 January 2014; accepted 22 August 2014
10.1126/science.1250744